J. Am. Chem. Soc. **1987**, *109*, 408-416

Ligand Perturbation of the Molecular and Electronic Structures of Quadruply Bonded Dimers. The Crystal Structures of $Mo_2Br_4(PMe_3)_4$ and $Mo_2I_4(PMe_3)_4$, and the Vibrational and Electronic Spectra of a Series of $M_2X_4L_4$ Complexes

Michael D. Hopkins,[1] William P. Schaefer,[1] Michael J. Bronikowski,[1] William H. Woodruff,[2] Vincent M. Miskowski,[1] Richard F. Dallinger,[2,3] and Harry B. Gray*[1]

Contribution No. 7398 from the Arthur Amos Noyes Laboratory, California Institute of Technology, Pasadena, California 91125, and the Isotope and Nuclear Chemistry Division, Los Alamos National Laboratory, Los Alamos, New Mexico 87545. *Received March 31, 1986*

Abstract: The ligand dependence of the molecular and electronic structures of quadruply bonded complexes of the $M_2X_4L_4$ type (M = Mo, W; X = Cl, Br, I; L = uncharged σ-donor ligand) has been investigated by evaluating four fingerprint experimental parameters: metal–metal distance and stretching frequency, and $^1(\delta \rightarrow \delta^*)$ transition energy and intensity. The metal–metal distances of $Mo_2Br_4(PMe_3)_4$ (2.125 (1) Å; space group $C2/c$, a = 18.472 (2) Å, b = 9.384 (2) Å, c = 17.519 (3) Å, β = 114.89 (1)°, V = 2755 (3) Å^3, and Z = 4) and $Mo_2I_4(PMe_3)_4$ (2.127 (1) Å; space group $P2_1/c$, a = 17.069 (3) Å, b = 10.784 (3) Å, c = 16.788 (3) Å, β = 105.39 (1)°, V = 2979 (2) Å^3, and Z = 4), in addition to that reported by Cotton et al. for $Mo_2Cl_4(PMe_3)_4$ (2.130 (0) Å), show an obvious indifference to the nature of the halide ligand. In contrast, the stretching frequencies ($\nu_1(Mo_2)$) associated with this internuclear separation, determined by resonance Raman spectroscopy, display a moderate ligand sensitivity: $\nu_1(X{=}Cl) = 355$, $\nu_1(Br) = 352$, $\nu_1(I) = 343$ cm^{-1}. Application of an empirical bond distance/force constant correlation leads to the conclusion that the effective reduced mass of the M–M unit increases according to Cl < Br < I and that G matrix mixing of M–M and M–X modes is appreciable. The frequencies of the latter mode for $Mo_2X_4(PMe_3)_4$ are the following: $\nu_2(X{=}Cl) = 274$, $\nu_2(Br) = 159$, $\nu_2(I) = 105$ cm^{-1}. The energies and intensities of the $^1(\delta \rightarrow \delta^*)$ transitions of the $Mo_2X_4(PMe_3)_4$ complexes display the largest ligand sensitivity of any of these parameters: X = Cl, $\bar{\nu}_{max}$ = 17 090 cm^{-1}, ϵ_{max} = 3110; X = Br, $\bar{\nu}$ = 16 720 cm^{-1}, ϵ = 4060; X = I, $\bar{\nu}$ = 15 720 cm^{-1}, ϵ = 5250 M^{-1}cm^{-1}. The second intense band in the visible absorption region is much more ligand sensitive ($\bar{\nu}_{max}$ = 25000–31000 cm^{-1}, ϵ_{max} = 3700–12000 M^{-1}cm^{-1}) and is assigned to $\sigma(MoP) \rightarrow \delta^*(Mo_2)$, although it also possesses substantial X → M charge-transfer character. The $^1(\delta \rightarrow \delta^*)$ parameters of the $Mo_2X_4(PMe_3)_4$ complexes are contrasted with those of other quadruply bonded dimers; attempts to reconcile these data with the spectral interpretations of Fackler et al. and Trogler et al. are not wholly successful. It is proposed that the intrinsic intensity of $^1(\delta \rightarrow \delta^*)$ is quite small ($\epsilon \sim 150$), with the observed intensity of halide-ligated dimers being dominated by stolen LMCT intensity. The spectral shifts of the $Mo_2X_4(PMe_3)_4$ series are consistent with configuration interaction with the intensity-giving charge-transfer state.

The results from electronic, vibrational, and photoelectron spectroscopy, in conjunction with X-ray crystallography, form the experimental foundation of our present understanding of the molecular and electronic structures of quadruply metal–metal bonded complexes.[4] Investigations employing these techniques have been directed at many members of this diverse set of compounds, and their findings have been of central importance in allowing the original qualitative bonding scheme proposed[5] for these systems to be significantly elaborated upon. Examination of the trends observed in these studies has, in addition, led to the delineation of several major electronic and structural subgroups of quadruply bonded complexes.[4] Metal dimers bridged by carboxylates, for example, are set apart from those ligated by halides in that they generally possess, for a given metal, shorter metal–metal bonds, higher frequency metal–metal stretching vibrations, and higher energy $^1(\delta \rightarrow \delta^*)$ electronic transitions. Electronic structural calculations, along with photoelectron spectroscopic experiments, have frequently been employed to elucidate the origin of such electronic differences; in the case of the carboxylate-bridged dimers they are proposed to arise from the mixing of orbitals associated with the M_2 unit with π-levels localized on the carboxylate moiety.[6]

Although the broad variations in the structural and electronic properties of homologous d^4-d^4 complexes of different metals, or of different ligand sets of the same dimetal unit, are well documented in many cases,[4] subtler perturbations resulting from ligand variation within a given subclass of dimers are less well understood. We have recently undertaken an investigation of the spectroscopic, magnetic, photophysical, and photochemical properties of a large number of derivatives of the $M_2X_4L_4$ type (M = Mo, W; X = Cl, Br, I; L = uncharged σ-donor ligand), which form one of the largest subclasses of quadruply bonded dimers. One of the more striking findings of these studies is that parameters such as $^1(\delta \rightarrow \delta^*)$ transition energies,[7] electronic absorption and emission band shapes and intensities,[7-9] and the rates of radiative and nonradiative excited state decay,[9] which are properties associated with the formally metal-metal-localized manifold of electronic states, display a marked sensitivity to the nature of ligands X and L. In order to determine whether this ligand dependence is also reflected in the ground-state properties of these complexes, as well as to provide a structural benchmark for analyzing ligand perturbations of their excited states, we determined the crystal structures of two such derivatives, $Mo_2Br_4(PMe_3)_4$ and $Mo_2I_4(PMe_3)_4$, and the

---

(1) California Institute of Technology.

(2) Los Alamos National Laboratory.

(3) Permanent address: Department of Chemistry, Wabash College, Crawfordsville, IN 47933.

(4) Cotton, F. A.; Walton, R. A. *Multiple Bonds Between Metal Atoms*; Wiley: New York, 1982.

(5) Cotton, F. A.; Curtis, N. F.; Harris, C. B.; Johnson, B. F. G.; Lippard, S. J.; Mague, J. T.; Robinson, W. R.; Wood, J. S. *Science* **1964**, *145*, 1305–1307.

(6) Norman, J. G., Jr.; Kolari, H. J. *J. Chem. Soc., Chem. Commun.* **1975**, 649–651. Norman, J. G.; Kolari, H. J.; Gray, H. B.; Trogler, W. C. *Inorg. Chem.* **1977**, *16*, 987–993.

(7) Hopkins, M. D.; Gray, H. B. *J. Am. Chem. Soc.* **1984**, *106*, 2468–2469.

(8) Miskowski, V. M.; Goldbeck, R. A.; Kliger, D. S.; Gray, H. B. *Inorg. Chem.* **1979**, *18*, 86–89.

(9) Zietlow, T. C.; Hopkins, M. D.; Gray, H. B. *J. Solid State Chem.* **1985**, *57*, 112–119.

0002-7863/87/1509-0408$01.50/0

vibrational and electronic spectra of a series of $M_2X_4L_4$ complexes. These results are reported herein, along with a general interpretation of the ligand sensitivity of the energies and intensities of the $^1(\delta \rightarrow \delta^*)$ transitions of quadruply bonded dimers.

Experimental Section

General Procedures. The preparations of the complexes described in this study were carried out on a high-vacuum manifold (limiting pressure $<10^{-3}$ torr) or with Schlenk techniques. Dichloromethane (Burdick and Jackson), benzene-d_6 (Aldrich), and 2-methylpentane (Phillips) were dried by standard methods,[10] degassed with five or more freeze-pump-thaw cycles, and stored under vacuum with, respectively, activated 4A molecular sieves, sodium metal/benzophenone, and lithium aluminum hydride. Trimethylphosphine (Strem) was degassed with 5 freeze-pump-thaw cycles and bulb-to-bulb distilled into an evacuated storage flask. All other chemicals were of reagent grade or comparable quality and were used as received. $Mo_2(O_2CCH_3)_4$,[11] $K_4Mo_2Cl_8$,[12] $W_2Cl_4(PMe_3)_4$,[13] and $Mo_2Cl_4(PMe_3)_4$[14] were prepared according to standard procedures. Elemental and mass spectral analyses were performed by Mr. Larry Henling at the Caltech Analytical Laboratory.

Electronic absorption spectra were recorded on either a Cary 17 or a Hewlett-Packard 8450A spectrometer. Spectra were obtained of solutions prepared on the vacuum line in a vessel consisting of a 10-mL round-bottomed flask, both 1 mm and 1 cm path length quartz spectral cells, and a Teflon high-vacuum stopcock. Solvent was first vacuum distilled from the appropriate storage flask to a calibrated volumetric cylinder and from there to the evacuated cell. The base lines of these spectra were corrected for the UV absorption of the solvent. Extinction coefficients were reproducible to ±2%. Oscillator strengths of absorption bands were determined by the cut-and-weigh method. ^{31}P NMR spectra were obtained of C_6D_6 solutions prepared and sealed under vacuum and recorded with a Jeol FX90Q FT-NMR spectrometer at 26 °C. Resonances are reported relative to external H_3PO_4 (aq). Magnetic susceptibilities were determined with an SHE 905 VTS SQUID susceptometer (10-kG field) of crystalline samples contained in an aluminum bucket of known magnetization. Raman spectra were recorded with one of two spectrometers: a Spex Ramalog EU equipped with a cooled RCA 31034A photomultiplier tube, an ORTEC 9300 series photon counter, and a Nicolet 1180E Raman data system; or a Spex 14024 spectrometer equipped with 2400 line/mm holographic gratings, a thermoelectric cooled Hamamatsu R955 photomultiplier tube, and a Spex SCAMP data system. Laser excitation was provided by either a Spectra-Physics 171-01(Kr^+) or 171-18(Ar^+) laser. Spectra were taken of both solutions and solids. The former were obtained in the rotating sample mode of N_2-purged solutions sealed in 5 mm diameter glass capillaries, while the latter were obtained of either polycrystalline samples mounted in an Air Products Displex cryostat at 20 K or of dilute KCl pellets at room temperature.

$Mo_2I_4(PMe_3)_4$. A vigorously stirred, 0 °C suspension of $Mo_2(O_2CCH_3)_4$ (1.67 g, 3.7 mmol) and trimethylphosphine (3 mL, 31.6 mmol) in 35 mL of dichloromethane was treated dropwise with Me_3SiI (5 g, 25.0 mmol), causing an immediate color change from bright orange to dark blue. The resulting suspension was stirred for 6 h at 0 °C and then allowed to warm slowly to room temperature, where it was stirred for an additional 24 h. The solvent was removed under vacuum, and the remaining blue-white inhomogeneous solid was extracted with toluene and filtered through a 3 × 20 cm column of 60–100 mesh Fluorisil. Vacuum evaporation of the solvent yielded 3.55 g (95%) of dark blue, microcrystalline $Mo_2I_4(PMe_3)_4$. Anal. Calcd (found) for $C_{12}H_{36}I_4P_4Mo_2$: C, 14.36 (14.26); H, 3.62 (3.47). ^{31}P NMR: δ −15.81 (s). $\chi_m(300\ K) = -333 \times 10^{-6}$; $\chi_m(6\ K) = -327 \times 10^{-6}$ emu/mol. This compound is air stable in the solid state and is soluble in hexane, benzene, dichloromethane, acetone, and, to a limited extent, methanol. It can be recrystallized from 4:1 dichloromethane:ethanol by evaporation; crystals suitable for X-ray diffraction studies were grown under nitrogen by slow evaporation of a hexane solution.

Table I. Crystal Data for $Mo_2Br_4(PMe_3)_4$ and $Mo_2I_4(PMe_3)_4$

	$Mo_2Br_4(PMe_3)_4$	$Mo_2I_4(PMe_3)_4$
formula weight	815.83	1003.81
space group	$C2/c$	$P2_1/c$
a, Å	18.472 (2)	17.069 (3)
b, Å	9.384 (2)	10.784 (3)
c, Å	17.519 (3)	16.788 (3)
β, deg	114.89 (1)	105.39 (1)
V, Å^3	2755 (3)	2979 (2)
Z	4	4
ρ_{calcd}, g cm^{-3}	1.97	2.24
$F(000)$, e$^-$	1548.9	1849.8
μ, cm^{-1}	72.7	23.36
crystal dimensions (mm)	0.15 × 0.20 × 0.24	0.16 × 0.17 × 0.27

Table II. Heavy-Atom Parameters for $Mo_2Br_4(PMe_3)_4$[a]

atom	x	y	z	U_{eq}[b]
Mo1	0	3321 (0.7)	$^1/_4$	296 (2)
Mo2	0	1057 (0.7)	$^1/_4$	285 (2)
Br1	−1085 (0.3)	4410 (0.7)	1184 (0.4)	528 (2)
Br2	−865 (0.3)	−20 (0.7)	3166 (0.4)	501 (2)
P1	930 (1)	3915 (2)	1803 (1)	468 (4)
P2	−1159 (1)	452 (1)	1109 (1)	427 (4)
C1	1970 (4)	3391 (8)	2320 (5)	752 (19)
C2	653 (4)	3416 (7)	723 (4)	664 (17)
C3	986 (4)	5858 (7)	1752 (4)	721 (20)
C4	−1234 (4)	−1482 (7)	1032 (4)	736 (22)
C5	−2157 (3)	969 (7)	956 (4)	593 (17)
C6	−1123 (4)	946 (7)	128 (4)	632 (19)

[a] All coordinates except Mo1(z) and Mo2(z) have been multiplied by 10^4. [b] $U_{eq} = {}^1/_3\sum_i\sum_j[u_{ij}(a_i^*a_j^*)(\vec{a}_i \cdot \vec{a}_j)]$; $\sigma(U_{eq}) = 6^{-1/2}\langle\sigma(U_{ii})/U_{ii}\rangle U_{eq}$.

$Mo_2Br_4(PMe_3)_4$. This compound was prepared and purified in high yield by the above procedure with Me_3SiBr as the bromide source. Anal. Calcd (found) for $C_{12}H_{36}Br_4P_4Mo_2$: C, 17.67 (17.80); H, 4.45 (4.32). ^{31}P NMR: δ −12.31 (s). Mass spectrum: m/z 816 (parent ion; relative intensity = 28), 740 (816 − PMe_3; 72), 664 (816 − $2PMe_3$; 100), 588 (816 − $3PMe_3$; 41), 508 (816 − $3PMe_3$ − Br; 13). Slow evaporation of a toluene solution of $Mo_2Br_4(PMe_3)_4$ yielded large (up to 5 mm in diameter), dark-red,[15] multifaceted prisms that were satisfactory for X-ray diffraction.

$Mo_2Cl_4(AsMe_3)_4$. A suspension of $K_4Mo_2Cl_8$ (0.75 g, 1.2 mmol) and trimethylarsine (1.5 mL, 14.1 mmol) in 50 mL of methanol was stirred at room temperature for 5 days. Although the color of the reaction mixture did not appear to change over this time period, irradiation of the flask with a UV lamp showed that the red-pink color of the contents was due to intense luminescence, which is absent in the starting material. The reaction mixture was filtered in air and the solid washed thoroughly with methanol, water (until the filtrate was colorless), and methanol again and dried in vacuo. Yield: 0.80 g (82%). Anal. Calcd (found) for $C_{12}H_{36}As_4Cl_4Mo_2$: C, 17.71 (17.83); H, 4.46 (4.27). The compound is stable to air in the solid state, although solutions decompose rapidly on exposure to oxygen.

X-ray Diffraction Procedures. Calculations for both structures were performed on a VAX 11/750 computer with the programs of the CRYRM Crystallographic Computing System. Scattering factors for neutral atoms and dispersion corrections for Mo, Br, and I were taken from the International Tables;[18] the function minimized in the least squares was $\sum w(F_o^2 - F_c^2)$, where $w = 1/\sigma^2(F_o^2)$.

Crystals that appeared single from oscillation photographs were centered on a CAD-4 diffractometer equipped with graphite-monochromated Mo Kα radiation (λ = 0.71073 Å). Collection of the data at room

---

(10) Perrin, D. D.; Armarego, W. L. F.; Perrin, D. R. *Purification of Laboratory Chemicals*; Pergamon: Oxford, 1966.

(11) Holste, G.; Schafer, H. *Z. Anorg. Allg. Chem.* **1972**, *391*, 263–270.

(12) Brencic, J. V.; Cotton, F. A. *Inorg. Chem.* **1970**, *9*, 351–353.

(13) Schrock, R. R.; Sturgeoff, L. G.; Sharp, P. R. *Inorg. Chem.* **1983**, *22*, 2801–2806. Sharp, P. R.; Schrock, R. R. *J. Am. Chem. Soc.* **1980**, *102*, 1430–1431.

(14) Cotton, F. A.; Extine, M. W.; Felthouse, T. R.; Kolthammer, B. W. S.; Lay, D. G. *J. Am. Chem. Soc.* **1981**, *103*, 4040–4045.

(15) Contrary to several reports of $Mo_2Cl_4(PMe_3)_4$[14,16] and $Mo_2Br_4(PMe_3)_4$[17b] existing as *dark blue* crystals, both materials are actually red as solids due to intense luminescence in room light.[7]

(16) Carmona, E.; Galindo, A.; Sanchez, L.; Nielson, A. J.; Wilkinson, G. *Polyhedron* **1984**, *3*, 347–352. Andersen, R. A.; Jones, R. A.; Wilkinson, G. *J. Chem. Soc., Dalton Trans.* **1978**, 446–453.

(17) (a) Following completion of this work a report of the synthesis and crystal structure of $Mo_2Br_4(PMe_3)_4$ appeared.[17b] Since the preparative route described by these workers is not as straightforward as that given here, and inasmuch as the crystallographic results are mentioned solely in the abstract of their paper, we present here the full details of our X-ray structure determination. Both crystal structures are in good agreement with respect to unit cell dimensions and bond distances and angles. (b) Ahmed, K. J.; Chisholm, M. H.; Huffman, J. C. *Organometallics* **1985**, *4*, 1168–1174.

(18) *International Tables for Crystallography*; Kynoch Press: Birmingham, England, 1974; Vol IV, pp 72 and 149.

(19) Main, P.; Hull, S. E.; Lessinger, L.; Germain, G.; De Clerq, J.-P.; Woolfson, M. M. *Multan 78*; University of York: York, England.

Table III. Heavy-Atom Parameters for $Mo_2I_4(PMe_3)_4$[a]

atom	x	y	z	U_{eq}[b] or B
Mo1	24236 (3)	54200 (5)	31439 (3)	353 (1)
Mo2	24984 (4)	43378 (5)	21077 (4)	374 (1)
I1	17014 (3)	77093 (5)	27795 (4)	597 (1)
I2	30622 (4)	43187 (7)	46411 (3)	769 (2)
I3	38846 (3)	46813 (6)	15815 (4)	722 (2)
I4	11813 (4)	28232 (6)	14775 (4)	747 (2)
P1	37478 (12)	66797 (25)	34863 (14)	643 (6)
P2	10519 (11)	47846 (19)	33810 (13)	488 (5)
P3	18449 (13)	57340 (20)	8782 (12)	518 (5)
P4	32035 (17)	23420 (21)	27568 (15)	700 (6)
C11	3916 (6)	7787 (9)	2745 (6)	6.5 (2)
C12	4712 (6)	5887 (10)	3811 (7)	7.1 (3)
C13	3794 (7)	7670 (10)	4369 (7)	7.8 (3)
C21	887 (5)	5611 (9)	4263 (6)	5.8 (2)
C22	128 (5)	5127 (8)	2587 (5)	5.3 (2)
C23	907 (5)	3207 (9)	3679 (6)	5.7 (2)
C31	786 (5)	6180 (9)	691 (5)	5.7 (2)
C32	1849 (6)	4927 (10)	−68 (6)	6.5 (2)
C33	2333 (5)	7176 (8)	744 (5)	5.3 (2)
C41	4239 (7)	2407 (11)	3416 (7)	8.3 (3)
C42	3292 (7)	1317 (11)	1922 (7)	7.8 (3)
C43	2708 (6)	1331 (11)	3336 (6)	7.6 (3)

[a] Coordinates of Mo, **I**, and P have been multiplied by 10^5. Coordinates of C and U_{eq} have been multiplied by 10^4. [b] $U_{eq} = {}^1/_3\sum_i\sum_j[U_{ij}(a_i^*a_j^*)(\vec{a}_i\cdot\vec{a}_j)]$; $\sigma(U_{eq}) = 6^{-1/2}\langle\sigma(U_{ii})/U_{ii}\rangle U_{eq}$.

temperature and refinement of the structures proceeded as follows.

$Mo_2Br_4(PMe_3)_4$:[17] A monoclinic cell was found similar to that of $Mo_2Cl_4(PMe_3)_4$,[14] and unit cell dimensions (Table I) were calculated from the setting angles of 25 reflections with $30° < 2\theta < 40°$. Data were collected for all $\pm h,k,l$ with $2\theta < 50°$. Altogether 2772 reflections were scanned in a θ–2θ mode, including 3 check reflections monitored every 5000 s of X-ray exposure time. The check reflections showed no variations greater than those expected from counting statistics. Lorentz and polarization factors were applied and a few duplicate reflections merged to give 2420 reflections that were used in the refinement. Variances were assigned to the values of F_o^2 based on counting statistics plus an additional term $(0.021I)^2$ to account for errors proportional to intensity. Systematic absences in the data were consistent with space group $C2/c$. Absorption corrections were not made because of the small size of the crystal ($\mu r_{max} = 1.3$).

The positional parameters of the $Mo_2Cl_4(PMe_3)_4$ structure[14] and reasonable isotropic thermal parameters served as the starting point of the refinement. The non-hydrogen atoms were given anisotropic thermal parameters after three cycles, and hydrogen atoms, positioned from difference Fourier maps, were included in the structure factor calculations after six cycles. The hydrogen atoms and their isotropic thermal parameters were not refined but were repositioned once. At convergence, $R = \sum|F_o - |F_c||/\sum F_o = 0.048$; the goodness of fit $[\sum w(F_o^2 - F_c^2)^2/(n - p)]^{1/2} = 2.37$, with $n = 2420$ data and $p = 106$ parameters. The final heavy-atom parameters for this compound are listed in Table II.

$Mo_2I_4(PMe_3)_4$: A monoclinic cell was found and cell dimensions (Table I) were calculated from the setting angles of 25 reflections with $21° < 2\theta < 27°$. Data were collected in the 2θ range 2–50° for all $\pm h,k,\pm l$. Altogether 10810 reflections were scanned in a θ–2θ mode, including 3 check reflections monitored every 10000 s of X-ray exposure time. The data were corrected for a slight linear decay and merged to give 5219 independent reflections, of which 4689 had $F_o^2 > 0$ and 4035 had $F_o^2 > 3\sigma(F_o^2)$. Variances were assigned the individual values of F_o^2 based on counting statistics plus an additional term, $0.014F_o^2$; variances of the merged reflections were obtained by standard propagation of error plus another additional term, $0.014\bar{F}_o^2$. Systematic absences in the data indicated space group $P2_1/c$ (# 14); assuming four molecules in the unit cell led to a reasonable density (2.24 g cm^{-3}). Again, no absorption corrections were made ($\mu r_{max} = 0.4$).

The structure was solved by Multan,[19] which gave the coordinates of the two molybdenum atoms and three of the iodine atoms. One structure factor-Fourier cycle led to the positions of the remaining nonhydrogen atoms. The hydrogen atoms were found in Fourier maps after six cycles of least squares, refining the positional parameters for all non-hydrogen atoms, anisotropic thermal parameters of Mo, I and P atoms, and isotropic thermal parameters of the carbon atoms in a single matrix. The hydrogen atoms were included as constant contributions in a final three cycles of least squares, with idealized C–H geometries and a thermal parameter equal to that of the carbon atom they were bonded to. At convergence, $R = \sum|F_o - |F_c||/\sum F_o = 0.048$ for all data with $F_o^2 > 0$ and 0.039 for the strong data. The goodness of fit, $[\sum w(F_o^2 - F_c^2)^2/(n - p)]^{1/2}$, is 2.38 for $n = 5219$ data and $p = 140$ parameters. A secondary extinction factor[20] was refined, with a final value of 0.34 (1) × 10^{-6}. The final heavy-atom parameters for this compound are set out in Table III.

Table IV. Bond Distances and Bond Angles of the $Mo_2X_4P_4$ Cores of $Mo_2Br_4(PMe_3)_4$ and $Mo_2I_4(PMe_3)_4$

Bond Distances

		distance (Å)	
atom	atom	X = Br	X = I
Mo1	Mo2	2.125 (1)	2.127 (1)
Mo1	X1	2.547 (1)	2.755 (1)
Mo1	X2		2.732 (1)
Mo1	P1	2.553 (2)	2.568 (2)
Mo1	P2		2.570 (2)
Mo2	X3	2.551 (1)	2.762 (1)
Mo2	X4		2.753 (1)
Mo2	P3	2.540 (2)	2.559 (2)
Mo2	P4		2.564 (3)

Bond Angles

			angle (deg)	
atom	atom	atom	X = Br	X = I
Mo2	Mo1	X1	113.65 (3)	115.5 (1)
		X2		114.7 (1)
		P1	102.60 (5)	103.5 (1)
		P2		103.6 (1)
Mo1	Mo2	X3	113.34 (3)	115.5 (1)
		X4		114.8 (1)
		P3	102.91 (4)	103.2 (1)
		P4		103.7 (1)

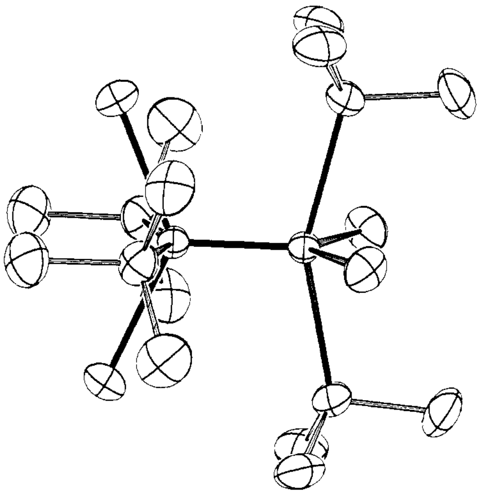

Figure 1. The molecular structure of the $Mo_2X_4(PMe_3)_4$ complexes, taken from the parameters for X = Br. This view, drawn by ORTEP, represents the projection of the structure onto the (101) face of the crystal.

Results and Discussion

Molecular Structures of $Mo_2X_4(PMe_3)_4$ (X = Cl, Br, I).[21] In view of the vast body of structural data on quadruply bonded complexes,[4] it is surprising that the crystallographic results reported here for $Mo_2Br_4(PMe_3)_4$ and $Mo_2I_4(PMe_3)_4$, along with that reported by Cotton et al. for $Mo_2Cl_4(PMe_3)_4$,[14] complete the first series for which the structures of homologous chloride-, bromide-, and iodide-containing dimers are known. The important bond distances and bond angles of the $Mo_2X_4P_4$ cores of $Mo_2Br_4(PMe_3)_4$ and $Mo_2I_4(PMe_3)_4$ are given in Table IV. As might be expected, all three compounds possess the idealized D_{2d} molecular symmetry usually found[22] for species of the $M_2X_4L_4$ type (Figure 1). The

---

(20) Larson, A. C. *Acta Crystallogr.* **1967**, *23*, 664–665, eq 3.

(21) Future references to the $Mo_2X_4(PMe_3)_4$ (X = Cl, Br, I) series as a whole will be given as $Mo_2X_4(PMe_3)_4$. The notation $M_2X_4L_4$ does not, however, restrict X to these three halides.

Table V. Average Bond Distances and Bond Angles of Selected $Mo_2X_4L_4$ Complexes

			distances (Å)			angles (deg)		
	X	L	M–M	M–X	M–L	MMX	MML	ref
(a)	Cl	PMe_3	2.130 (0)	2.414 (1)	2.545 (1)	112.2 (1)	102.3 (1)	14
	Br	PMe_3	2.125 (1)	2.549 (1)	2.547 (2)	113.5 (1)	102.8 (1)	*b*
	I	PMe_3	2.127 (1)	2.751 (1)	2.565 (2)	115.1 (1)	103.5 (1)	*b*
(b)	CH_3	PMe_3	2.153 (1)	2.439 (5)	2.513 (2)	115.3 (1)	102.5 (5)	24
	Cl	SMe_2	2.144 (1)	2.404 (2)	2.530 (2)	108.7 (1)	98.4 (1)	23
	OCH_2-*t*-Bu	PMe_3	2.209 (1)	2.03 (2)	2.54 (2)	110	*a*	31

[a] Not reported. [b] This work.

principal crystallographic difference among these halogen derivatives is that the iodide adduct crystallizes in a lower symmetry space group ($P2_1/c$) than do the isomorphous ($C2/c$) chloride and bromide complexes, although examination of the former's symmetry-unrelated metal–ligand bond distances and bond angles (Table IV) shows that its geometry is nonetheless very regular. In fact, even though the crystallographically imposed symmetries of $Mo_2Br_4(PMe_3)_4$ and $Mo_2I_4(PMe_3)_4$ are C_2 and C_s, respectively, the overall deviations of their $Mo_2X_4P_4$ cores from D_{2d} symmetry are quite small.

Comparison of the molecular structures of these halide derivatives of $Mo_2X_4(PMe_3)_4$ affords an interesting opportunity to gauge the effects on the metal–metal bond of systematic steric and inductive perturbations by these ligands. The average bond distances and bond angles of $Mo_2X_4(PMe_3)_4$ are listed in Table Va. Most noteworthy is the fact that the metal–metal distances of these species are independent of the nature of X across this series, spanning a range of only 0.005 Å. These distances are comparable to those of the related $Mo_2Cl_4(SMe_2)_4$[23] and $Mo_2(CH_3)_4(PMe_3)_4$[24] compounds (Table Vb) and are well within the range considered normal for complexes containing the Mo_2^{4+} unit.[4] It is clear from these results that structural accommodation of the increasing interligand repulsion in the series Cl < Br < I does not occur along the metal–metal bond for complexes of this type, instead being reflected solely in their metal–ligand bond distances and bond angles. Specifically, the differences between the lengths of the metal halide bonds in this series are (d(MoBr) − d(MoCl)) = 0.135 Å and (d(MoI) − d(MoBr)) = 0.202 Å, in reasonable agreement with the corresponding differences between the ionic radii of these halides, namely $r_{Br} - r_{Cl} = 0.15$ Å and $r_I - r_{Br} = 0.24$ Å.[25] In addition, there are small increases in both the Mo–Mo–X and Mo–Mo–P bond angles in the order Cl < Br < I, although the former only changes by 3° across this series and the latter by slightly over 1°, as well as a small lengthening (0.02 Å) of the Mo–P bond of the iodide adduct relative to the chloride and bromide derivatives.[26]

Although the structural insensitivity of the metal–metal bond to the nature of the halogen ligand seems reasonably accounted for by the small perturbations to the metal–ligand environment of these systems, the electronic interpretation of this finding is less straightforward. The electronic structures of the model systems $Mo_2Cl_4(PH_3)_4$ and $W_2Cl_4(PH_3)_4$ have been previously investigated by SCF–Xα–SW calculations.[28] Of primary importance to this discussion is the fact that the metal-localized δ- and π-bonding levels possess, at least at this level of theory, non-negligible halogen orbital character.[29] Given the increasing ligand polarizability in the series Cl < Br < I, it seems very likely that the metal–metal bonding levels of all three derivatives undergo, to quite different extents, strong metal–halide orbital mixing, with increasing ligand–d-orbital participation along this series.[30] That metal–ligand π-interactions can be sufficiently strong to influence the extent of metal–metal bonding is demonstrated by $Mo_2(OCH_2$-*t*-$Bu)_4(PMe_3)_4$[31] (Table Vb), whose internuclear separation is the longest known for a dimolybdenum quadruple bond, being nearly 0.1 Å longer than those of the halide derivatives. In this instance, substantial multiple bond character is attributed to the Mo–O bond, with this repolarization of the d-electron density of the metals resulting in a significantly weakened metal–metal bond.[31,32] We see no simple explanation for the total absence of such structural changes in the case of the halogen adducts, except to note that less dramatic perturbations of metal–metal overlap may not manifest themselves in the metal–metal bond length. We are currently pursuing this problem further by examining the photoelectron spectrum of $Mo_2Br_4(PMe_3)_4$ for the purpose of comparison with that reported[28] for $Mo_2Cl_4(PMe_3)_4$.

Vibrational Spectroscopy. Several detailed studies of the Raman spectroscopy of the $Mo_2X_8^{4-}$ (X = Cl, Br) ions have demonstrated that these species exhibit strong resonance enhancement of the totally symmetric $\nu_1(Mo_2)$ vibration upon excitation into the $^1(\delta \rightarrow \delta^*)$ absorption band, as is dramatically manifested in the spectra of these complexes by long overtone progressions (up to $11\nu_1$) in this mode.[33-35] Resonance Raman (RR) spectral data have also been reported for over 20 $Mo_2X_4L_4$ complexes,[36-38] and although they display much shorter progressions ($\leq 3\nu_1$) in the $a_1\nu_1(Mo_2)$ mode, this frequency has been clearly identified in every instance, falling in the range $330 \leq \nu_1 \leq 358$ cm^{-1}. Since for only one of these latter complexes were both the metal–metal distance and its corresponding stretching frequency known, we obtained RR spectra for the structurally characterized $Mo_2X_4(PMe_3)_4$ series in order to facilitate comparisons among these systems.

---

(22) Two centrosymmetric (D_{2h}) species, Mo_2X_4(4-picoline)$_4$ (X = Cl, Br), have been structurally characterized (Brencic, J. V.; Golic, L.; Leban, I.; Segedin, P. *Monatsh. Chem.* **1979**, *110*, 1221–1228).

(23) Cotton, F. A.; Fanwick, P. E. *Acta Crystallogr.* **1980**, *B36*, 457–459. Marsh, R. E. *Acta Crystallogr.* **1981**, *B37*, 1985–1988.

(24) Girolami, G. S.; Mainz, V. V.; Andersen, R. A.; Vollmer, S. H.; Day, V. W. *J. Am. Chem. Soc.* **1981**, *103*, 3953–3955.

(25) Weast, R. C., Ed. *CRC Handbook of Chemistry and Physics*, 58th ed.; CRC Press: Cleveland, 1977; p F-213.

(26) We note here, as others have previously on related systems,[14,27,28] that the Mo–P bonds of $Mo_2X_4(PMe_3)_4$ appear to be anomalously long relative to the Mo–X bonds. Comparison of these distances in $Mo_2Cl_4(PMe_3)_4$ (d(Mo–Cl) = 2.414 (1) Å, d(Mo–P) = 2.545 (1))[14] to those reported for its most closely related monomeric analogue, *trans*-$MoCl_2(PMe_3)_4$ (2.420 (6) and 2.496 (3), respectively) (Carmona, E.; Marin, J. M.; Poveda, M. L.; Atwood, J. L.; Rogers, R. D. *Polyhedron* **1983**, *2*, 185–193) serves to illustrate this point clearly. Some discussion of this result in the context of an SCF–Xα–SW calculation has been offered elsewhere.[28]

(27) Cotton, F. A.; Felthouse, T. R. *Inorg. Chem.* **1981**, *20*, 3880–3886.

(28) Cotton, F. A.; Hubbard, J. L.; Lichtenberger, D. L.; Shim, I. *J. Am. Chem. Soc.* **1982**, *104*, 679–686.

(29) Atomic contributions (percent):[28] $\delta(Mo_2)$ (72 Mo, 14 Cl, 1 P); $\pi(Mo_2)$ (52 Mo, 32 Cl, 8 P); σ(MoP) (18 Mo, 11 Cl, 48 P).

(30) Mixing of halide d orbitals with the δ and δ^* levels of $Mo_2X_4(PMe_3)_4$ has been invoked to explain trends in the oxidation and reduction potentials of these complexes that are "inverted" relative to those predicted from electronegativity arguments. (Zietlow, T. C.; Hopkins, M. D.; Gray, H. B. *J. Am. Chem. Soc.*, in press.)

(31) Chisholm, M. H.; Folting, K.; Huffman, J. C.; Tatz, R. J. *J. Am. Chem. Soc.* **1984**, *106*, 1153–1154.

(32) Coffindaffer, T. W.; Niccola, G. P.; Powell, D.; Rothwell, I. P.; Huffman, J. C. *J. Am. Chem. Soc.* **1985**, *107*, 3572–3583.

(33) Angell, C. L.; Cotton, F. A.; Frenz, B. A.; Webb, T. R. *J. Chem. Soc., Chem. Commun.* **1973**, 399–400. Clark, R. J. H.; Franks, M. L. *J. Chem. Soc., Chem. Commun.* **1974**, 316–317.

(34) Clark, R. J. H.; Franks, M. L. *J. Am. Chem. Soc.* **1975**, *97*, 2691–2697.

(35) Clark, R. J. H.; D'Urso, N. R. *J. Am. Chem. Soc.* **1978**, *100*, 3088–3091.

(36) San Filippo, J., Jr.; Sniadoch, H. J. *Inorg. Chem.* **1973**, *12*, 2326–2333.

(37) San Filippo, J., Jr.; Sniadoch, H. J.; Grayson, R. L. *Inorg. Chem.* **1974**, *13*, 2121–2130.

(38) Ribas, J.; Jugie, G.; Poilblanc, R. *Trans. Met. Chem.* **1983**, *8*, 93–98.

Table VI. Solid-State Resonance Raman Data for $Mo_2X_4L_4$ Complexes^a

Fundamentals							
$Mo_2Cl_4(AsMe_3)_4$^{c,d}		$Mo_2Cl_4(PMe_3)_4$^{b,e,f}		$Mo_2Br_4(PMe_3)_4$^{b,e}		$Mo_2I_4(PMe_3)_4$^{b,f,g}	
A1.	107 m	A2.	108 w	A3.	106 w	A4.	105 w (ν(MoI))
B1.	123 m	B2.	134 m	B3.	159 m (ν(MoBr))	B4.	148 w
C1.	152 w	C2.	153 w	C3.	209 w	C4.	163 w
D1.	217 w (ν(MoAs))	D2.	165 w	D3.	228 w	D4.	207 m
E1.	278 m^h (ν(MoCl))	E2.	215 w	E3.	235 w (ν(MoP))	E4.	219 w
F1.	337 w	F2.	235 w (ν(MoP))	F3.	270 w	F4.	248 m (ν(MoP))
G1.	356 vs^h (ν(Mo_2))	G2.	250 w	G3.	279 w	G4.	275 w
H1.	591 m (ν(AsC))	H2.	262 w	H3.	296 w	H4.	286 w
I1.	610 m (ν(AsC))	I2.	274 m^h (ν(MoCl))	I3.	337 w	I4.	343 vs^h (ν(Mo_2))
J1.	618 w (ν(AsC))	J2.	338 m^h	J3.	352 vs^h (ν(Mo_2))	J4.	720 w (ν(PC))
K1.	1448 w (δ(CH_3))	K2.	355 vs^h (ν(Mo_2))	K3.	740 w (ν(PC))	K4.	737 w (ν(PC))
		L2.	746 w (ν(PC))				
Resonance Raman Overtones and Combinations							
	466 (G1 + A1)		450		483		441 (I4 + A4)
	478^h (G1 + B1)		476		510 (J3 + B3)		487 (I4 + B4)
	510 (G1 + C1)		507 (K2 + C2)		602		500 (I4 + C4)
	635^h (G1 + E1)		550		620 (J3 + F3)		553 (I4 + D4)
	710^h (2G1)		618		675 (J3 + I3)		597
	815 (2G1 + A1)		683^h (2I4)		706^h (2J3)		683^h (2I4)
	832 (2G1 + B1)		710^h (2K2)		785		782 (2I4 + A4)
	855 (2G1 + C1)		1060^h (3K2)		808		845 (2I4 + C4)
	990 (2G1 + E1)				950		892 (2I4 + D4)
	1063^h (3G1)				967 (2J3 + F3)		1045^h (3I4)
	1153				1023		
	1173 (3G1 + A1)				1056^h (3J3)		
	1187				1293		
	1205				1405 (4J3)		
	1218				1515		
	1263				1532		
	1310				1580		
	1328				1600		
	1368				1652		
	~1410^h (4G1)				1755 (5J3)		
					~2105 (6J3)		

^{a}Frequencies are in cm^{-1}. ^{b}Polycrystalline solid, 20 K. ^{c}KCl pellet, 300 K. ^{d}λ_{ex} = 514.5 nm. ^{e}λ_{ex} = 520.8 nm. ^{f}λ_{ex} = 530.9 nm. ^{g}λ_{ex} = 568.2 nm. ^{h}Also observed in benzene solution at room temperature.

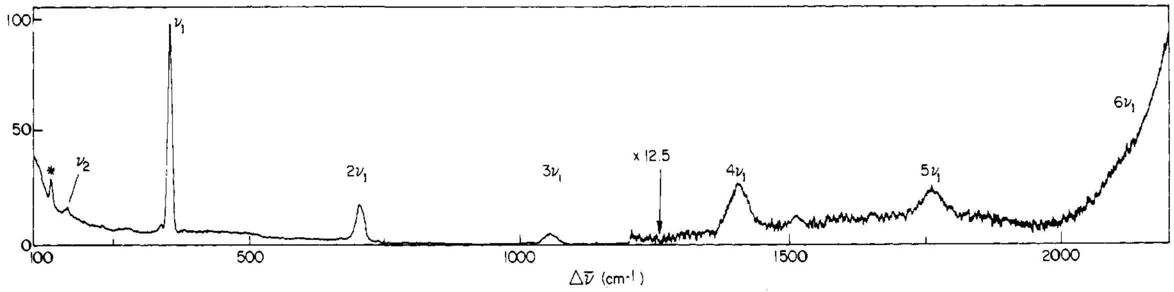

Figure 2. Raman spectrum of polycrystalline $Mo_2Br_4(PMe_3)_4$ at ca. 20 K (λ_{ex} = 530.9 nm). The peak marked with an asterisk is a laser plasma line.

The RR data for $Mo_2X_4(PMe_3)_4$ and $Mo_2Cl_4(AsMe_3)_4$ obtained upon excitation into their $^1(\delta\rightarrow\delta^*)$ absorption bands (vide infra) are given in Table VI.[39] In benzene solution the extremely strong $a_1\nu_1(Mo_2)$ fundamental for the chloride, bromide, and iodide derivatives of $Mo_2X_4(PMe_3)_4$ is observed at 355, 352, and 343 cm^{-1}, respectively, and that for $Mo_2Cl_4(AsMe_3)_4$ is seen at 356 cm^{-1}. In each instance, two or three overtones of this mode are also observed. The bands attributable to ν_1 are polarized, with the depolarization ratios of the fundamental of this mode for $Mo_2Cl_4(PMe_3)_4$ and $Mo_2Br_4(PMe_3)_4$ being ρ = 0.33 and 0.34, respectively, upon excitation at 514.5 nm, in perfect agreement with the value of $^1/_3$ expected for a totally symmetric vibration of a linear oscillator in resonance with an electronic transition between nondegenerate states ($\alpha_{zz} \gg \alpha_{xx} = \alpha_{yy}$).[40] RR spectra obtained of polycrystalline samples of these four complexes at low temperature are qualitatively similar to their solution counterparts, and although they display more and sharper bands, corresponding features between the two sets of spectra seldom differ in frequency by greater than 1 cm^{-1}. The most noticeable improvement in the quality of these spectra arises from a red shift of the fluorescence background, allowing longer overtone progressions in ν_1 to be observed. The low-temperature RR spectrum of polycrystalline $Mo_2Br_4(PMe_3)_4$ (Figure 2) is typical in this regard, showing the sharp fundamental at 352.9 cm^{-1}, along with five overtones before the onset of fluorescence. Calculation of the harmonic frequency and anharmonicity constant for this compound from the frequencies of $1\nu_1$–$5\nu_1$ indicates that this vibration is highly harmonic, these values being ω_{11} = 352.6 cm^{-1} and χ_{11} = −0.2 cm^{-1}, respectively. While comparable data for other $Mo_2X_4L_4$ systems have not yet been reported, the magnitude of this anharmonicity

---

[39] Although the intense fluorescence of these complexes[7] required excitation wavelengths to be significantly blue-shifted from the $^1(\delta\rightarrow\delta^*)$ λ_{max} in order for usable base lines to be obtained, resonance enhancement is nonetheless observed.

[40] Clark, R. J. H.; Stewart, B. *Struct. Bonding* **1979**, *36*, 1–80.

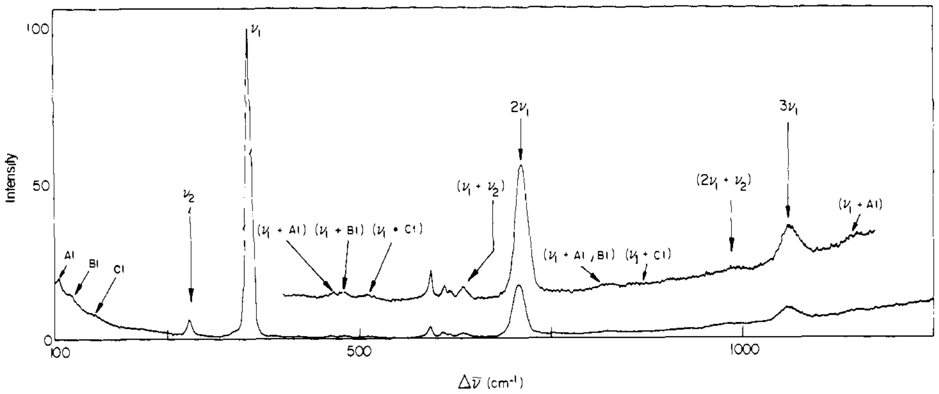

Figure 3. Raman spectrum of a KCl pellet of $Mo_2Cl_4(AsMe_3)_4$ at room temperature (λ_{ex} = 514.5 nm).

is in good agreement with those of the $Mo_2X_8^{4-}$ ions,[34,35] and is probably typical for the metal–metal vibrations of the $Mo_2X_4L_4$ class as a whole.

In addition to displaying bands attributable to the $a_1\nu_1(Mo_2)$ mode, the RR spectra of these complexes contain a number of lines arising from both metal–ligand and ligand-localized vibrations (Table VI). Few of these bands are very intense, however, and most are observed only in the solid-state spectra; in the absence of depolarization ratios and isotopic shift data, definitive assignments for these modes cannot, for the most part, be offered here, nor have they been assigned in previous studies of these complexes.[36–38] The solid-state RR spectrum of $Mo_2Cl_4(AsMe_3)_4$, reproduced in Figure 3, illustrates the low intensity of these bands relative to ν_1. The band at 278 cm^{-1} in this spectrum, which is the most intense of the low-frequency lines, and one of comparable intensity observed for $Mo_2Cl_4(PMe_3)_4$ at 274 cm^{-1}, are assigned to the totally symmetric metal–halide stretch ($a_1\nu_2$(MoX)) by analogy to the assignment for $Mo_2Cl_8^{4-}$, whose various salts display this band between 270 and 280 cm^{-1}.[34] Previously unassigned lines reported for $Mo_2Cl_4L_4$ (L = P-*n*-Bu_3,[36] SMe_2,[37] SEt_2,[37] $AsEt_3$[38]) in the 277–285-cm^{-1} range are probably also attributable to this vibration. The band at 159 cm^{-1} in the spectrum of $Mo_2Br_4(PMe_3)_4$ (Figure 2), while slightly weaker than its counterparts in the chloride spectra, is similarly assigned to ν_2; the corresponding frequency for $Mo_2Br_8^{4-}$ is 169 cm^{-1},[35] and $Mo_2Br_4(AsEt_3)_4$ shows a weak line at 170 cm^{-1}.[38] As has been observed for the $Mo_2X_8^{4-}$ ions,[34,35] the spectra of both $Mo_2Br_4(PMe_3)_4$ and $Mo_2Cl_4(AsMe_3)_4$ display the combination band of this mode with ν_1, with the latter complex additionally showing a combination tone progressing in ν_1 ($2\nu_1 + \nu_2$; Figure 3).

In contrast to those of the chloride and bromide complexes, the RR spectrum of $Mo_2I_4(PMe_3)_4$ displays only weak lines of nearly equal intensity in the low frequency region.[41] Empirical force constant/bond distance correlations[43] predict a frequency of 128 cm^{-1} for the Mo–I stretch from its bond distance. Since similar calculations for the chloride and bromide complexes predict Mo–X stretching frequencies that are approximately 10% higher than those observed experimentally, a value near 110 cm^{-1} is reasonable for ν(MoI). A similar value is estimated by comparing the M–X frequencies of $Re_2X_8^{2-}$[42] to those of $Mo_2Cl_4L_4$ and $Mo_2Br_4(PMe_3)_4$ and extrapolating to $Mo_2I_4(PMe_3)_4$. The only RR mode near this frequency for the iodide compound is at 105 cm^{-1} (Table VI). While peaks at similar frequencies also occur in the chloride and bromide derivatives, the 105-cm^{-1} mode of $Mo_2I_4(PMe_3)_4$ is unique among the $Mo_2X_4(PMe_3)_4$ complexes in that it forms combination tones with the ν_1 progression (ν_1 + 105 and $2\nu_1$ + 105), as observed for the Mo–X stretches in other $Mo_2X_4L_4$ complexes, and in the spectra of quadruply bonded halide complexes in general.[33–38] Therefore, we assign the 105-cm^{-1} peak as $a_1\nu_2$(MoI).[44,45]

With respect to drawing structural conclusions from comparisons of the vibrational frequencies of these complexes, it should be noted that the fact that the $Mo_2X_4(PMe_3)_4$ complexes display different frequencies for ν_1, even though they possess a single metal–metal distance, indicates that this vibration is not purely metal–metal stretching in nature. The empirical force constant/bond distance correlations referred to above can be used to calculate bond distances from the vibrational data given a reliable determination of the force constant. In many systems, especially metal–metal bonded complexes wherein the equatorial metal–ligand bonds are at approximately 90° to the metal–metal axis,[46,47] the diatomic approximation ($F = (5.9 \times 10^{-7})\mu\nu^2$ mdyn/Å) is sufficiently accurate to permit the estimation of metal–metal distances from $\nu_1(M_2)$ with a precision of ±(0.02–0.03)Å.[43] The appropriate function for the second transition series is $r(\text{Å}) = 1.83 + 1.51[\exp(-F/2.48)]$.[43] Application of these expressions to the $Mo_2X_4(PMe_3)_4$ complexes yields Mo–Mo distances of 2.19 Å (X = Cl, Br) and 2.22 Å (X = I), unacceptably higher than the crystallographically determined distance of 2.13 Å for all three complexes. Since the MoMoX angles in these species are significantly greater than 90° (113–115°; Table V), the diatomic approximation for extracting the metal–metal force constant is inaccurate for two reasons: the effective reduced mass of the M–M system increases because of contributions from the ligand masses; and G matrix mixing of the M–M and M–X coordinates becomes appreciable.[46] Both of these effects will tend to make the frequency of the (predominantly) M–M coordinate lower than that dictated by the diatomic approximation for a given M–M force constant; this is the direction of the error in the empirical bond distances in the present case. Thus, comparisons of simple diatomic force constants among complexes containing different ligand sets, or for homologous complexes of different metals,[48] must be viewed with caution in seeking meaningful information regarding the relative metal–metal bonding in these systems. On the other hand, vibrational analyses of these systems will provide more realistic force constants and lead to more rigorous tests of the empirical relationship,[43] which appears to be valid for all modes of bonding.

Electronic Spectroscopy. The room temperature solution spectra of $Mo_2X_4(PMe_3)_4$ and $Mo_2Cl_4(AsMe_3)_4$ are reproduced in Figure

---

(41) A similar observation has been reported for $Re_2I_8^{2-}$,[42] for which the intensity of ν_2 is much weaker than the corresponding modes of $Re_2X_8^{2-}$ (X = F, Cl, Br) upon $^1(\delta{\rightarrow}\delta^*)$ excitation.

(42) Clark, R. J. H.; Stead, M. J. *Inorg. Chem.* **1983**, *22*, 1214–1220.

(43) Woodruff, W. H., to be submitted for publication.

(44) Strong resonance enhancement of metal–ligand vibrational modes has been observed for the $Re_2X_8^{2-}$ ions upon excitation into the LMCT transitions of these complexes.[42] In an attempt to obtain depolarization ratios of these modes for the $Mo_2X_4L_4$ complexes, we acquired Raman spectra of benzene solutions of $Mo_2Cl_4(PMe_3)_4$ and $Mo_2Br_4(PMe_3)_4$ using excitation lines of 351.1 and 363.8 nm, respectively, which are in close proximity to LMCT bands of these species (vide infra). The spectrum of the chloride derivative displayed only ν_1 and ν_2, with roughly equal intensity, while the bromide showed only ν_1; these lines were very weak, and no overtones were observed.

(45) Detailed assignments of the remaining weak bands in the Raman spectra presented here, as well as those observed in the far-infrared spectra of these species, will be published separately: Hopkins, M. D.; Woodruff, W. H.; Gray, H. B., to be submitted for publication.

(46) Bratton, W. K.; Cotton, F. A.; Debeau, M.; Walton, R. A. *J. Coord. Chem.* **1971**, *1*, 121–131.

(47) Hutchinson, B.; Morgan, J.; Cooper, C. B., III; Mathey, Y.; Shriver, D. F. *Inorg. Chem.* **1979**, *18*, 2048–2049.

(48) Reference 4, p 428.

Table VII. Electronic Absorption Data for $M_2X_4L_4$ Complexes[a]

	compound	band I [$^1(\delta\rightarrow\delta^*)$]				band II [LMCT]			ref
		$\bar{\nu}$, cm^{-1}		ε, M^{-1} cm^{-1}	*f*	$\bar{\nu}$, cm^{-1}		ε, M^{-1} cm^{-1}	
(a)	$Mo_2Cl_4(AsMe_3)_4$	17420		2970	0.023	30960		3630	*b*
	$Mo_2Cl_4(PMe_3)_4$	17090	370	3110	0.024	30860	1870	3720	*b*
	$Mo_2Br_4(PMe_3)_4$	16720	1000	4060	0.030	28990	3670	6650	*b*
	$Mo_2I_4(PMe_3)_4$	15720		5250	0.040	25320		11850	*b*
(b)	$Mo_2Cl_4(P\text{-}n\text{-}Bu_3)_4$	17040		3150	0.026	30490		3830	8
	$W_2Cl_4(PMe_3)_4$	15150		4170	0.028	34130		9090	*b*
	$\beta\text{-}Mo_2Cl_4(dmpe)_2$	12450		210	0.0018	29150		3660	60

[a] Bands I and II are shown in Figures 4 and 5. [b] This work.

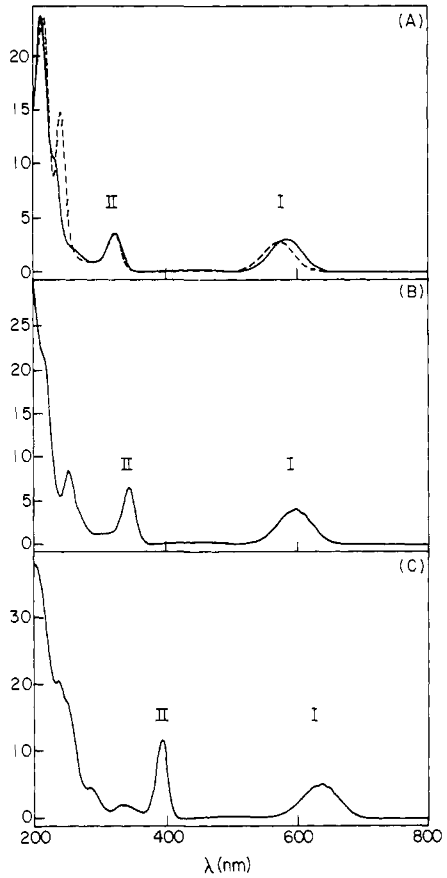

Figure 4. Electronic absorption spectra of $Mo_2X_4L_4$ in 2-methylpentane solution at room temperature: (a) X = Cl, L = PMe_3 (—); X = Cl, L = $AsMe_3$ (---); (b) X = Br, L = PMe_3; (c) X = I, L = PMe_3.

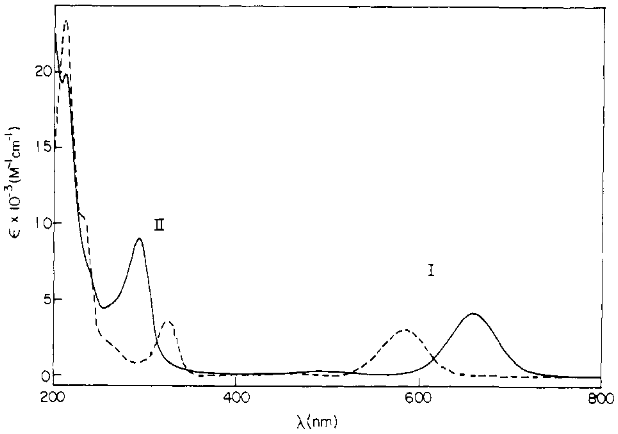

Figure 5. Electronic absorption spectra of $M_2Cl_4(PMe_3)_4$ in 2-methylpentane solution at room temperature: M = Mo (---); M = W (—).

4, and that of $W_2Cl_4(PMe_3)_4$ is shown in Figure 5. The visible absorption region of each spectrum displays three distinct band systems: two strong absorptions, which will be discussed shortly and are labeled I and II, and a weak cluster of bands, located between I and II.[49] To higher energy of band II, these spectra display a pattern of absorptions too complex to allow simple correlations between individual bands in the absence of a more detailed spectroscopic study. These transitions remain unassigned at this time, although we note that the similarity of the UV spectra of $Mo_2Cl_4(PMe_3)_4$ and $Mo_2Cl_4(AsMe_3)_4$, as well as the increasing complexity in this region according to Cl < Br < I, is undoubtedly a reflection of the lowering in energy of the numerous X → M charge-transfer transitions that these species possess. The intense, metal–metal-localized $^1(\pi\rightarrow\pi^*)$ transition should also be observed in this energy region.[50]

The energies and extinction coefficients of bands I and II for $Mo_2X_4(PMe_3)_4$ and $Mo_2Cl_4(AsMe_3)_4$ are summarized in Table VIIa. Band I of $Mo_2X_4L_4$ has been conclusively assigned to the $^1(\delta\rightarrow\delta^*)$ transition on the basis of a detailed spectroscopic study.[7,49] What is noteworthy in the context of the current discussion is that this band displays a marked sensitivity to the nature of ligand X, systematically both red-shifting and increasing in intensity for $Mo_2X_4(PMe_3)_4$ according to Cl < Br < I. The extinction coefficient of this band for $Mo_2I_4(PMe_3)_4$ is substantially larger than any previously reported for a quadruply bonded complex.[51] Band I is relatively insensitive to ligand L, in contrast, displaying similar intensities for the PMe_3, $AsMe_3$ (Table VIIa), and P-*n*-Bu_3 (Table VIIb) adducts of $Mo_2Cl_4L_4$; the spectra of the two phosphine derivatives are virtually superimposable, in fact, while the arsine complex displays a slight blue shift. Finally, the $^1(\delta\rightarrow\delta^*)$ absorption both red-shifts (1940 cm^{-1}) and increases in intensity upon going from $Mo_2Cl_4(PMe_3)_4$ to $W_2Cl_4(PMe_3)_4$ (Figure 5, Table VIIb). Band II displays relative sensitivities toward X and L for $Mo_2X_4L_4$ similar to those observed for band I, although its dependence on X is much greater than that of $^1(\delta\rightarrow\delta^*)$. Specifically, the red shift of band II across the Cl, Br, I series is 5540 cm^{-1}, which is four times greater than that for band I. In addition, the extinction coefficient of this band triples as a result of this perturbation, while that of band I increases, in comparison, by ~60%. The full width at half maximum (fwhm), which is independent of halide for the $^1(\delta\rightarrow\delta^*)$ transition, decreases significantly across this series: X = Cl, fwhm = 2600; X = Br, 2030; X = I, 1420 cm^{-1}. As is observed for band I, though, band II is little affected by the nature of L, again as illustrated by the close similarity of the $Mo_2Cl_4L_4$ (L = PMe_3, P-*n*-Bu_3, $AsMe_3$) spectra. On substitution of tungsten for molybdenum in $M_2Cl_4(PMe_3)_4$, band II increases in intensity by 2.5 times and, in contrast to band I, blue-shifts (3270 cm^{-1}) (Figure 5).

The large difference in the sensitivity of the position, intensity, and width of band II toward X relative to that of the $^1(\delta\rightarrow\delta^*)$ transition suggests that this band, in contrast, is not attributable to a transition between orbitals associated with the metal–metal

---

[49] These weak absorptions have been assigned on the basis of a low-temperature polarized single-crystal spectroscopic study that will be published separately. Hopkins, M. D.; Miskowski, V. M.; Gray, H. B., to be submitted for publication.

[50] Trogler, W. C.; Gray, H. B. *Acc. Chem. Res.* **1978**, *11*, 232–239.

[51] Reference 52, Table XIII.

[52] Manning, M. C.; Trogler, W. C. *J. Am. Chem. Soc.* **1983**, *105*, 5311–5320.

bond framework. Instead, the red shift of this band across the Cl, Br, I series, and its blue shift for the Mo → W perturbation, is entirely consistent with its assignment to an LMCT transition. The lowest energy transition of this type predicted by SCF-Xα-SW and LCAO-HFS transition-state calculations on $Mo_2Cl_4(PH_3)_4$[28,53] and $W_2Cl_4(PH_3)_4$[28] is $\sigma(M-P) \rightarrow \delta^*(M_2)$ in both instances. This is not an unreasonable assignment for these complexes given the close similarity of this band for $Mo_2Cl_4(PMe_3)_4$ and $Mo_2Cl_4(AsMe_3)_4$[54] and the relative weakness of the Mo–P bond,[26] as well as the fact that the red shift of the lowest lying $\pi(X) \rightarrow \delta^*(M_2)$ absorption of $Re_2X_8^{2-}$ along this series (Cl → Br: 7000; Br → I: 9000 cm^{-1})[42] is substantially larger than that seen for $Mo_2X_4(PMe_3)_4$ (Table VIIa). The strong perturbation of the energy and intensity of this absorption upon exchanging bromide or iodide for chloride suggests, however, that this excited state increasingly mixes with X → M states along this series,[29] with $\pi(X) \rightarrow \delta^*(Mo_2)$ perhaps becoming the dominant contributor to the lowest energy charge transfer state of the iodide complex.

The Energies and Intensities of $^1(\delta \rightarrow \delta^*)$ Transitions. The most obvious question to arise from consideration of the spectral data of the $Mo_2X_4(PMe_3)_4$ series is why the close similarity of the metal–metal bonding in these complexes that is suggested by their crystal structures is not reflected in the energies and intensities of their $^1(\delta \rightarrow \delta^*)$ transitions. The energy and intensity of this band must reflect, for a given complex, the extent of δ-bonding in that system inasmuch as the magnitudes of these parameters are determined in part by the energetic splitting of the one-electron δ and δ* levels and the square of the δ-overlap, respectively:[50] can comparisons of these parameters for different complexes, such as the $Mo_2X_4(PMe_3)_4$ series, provide a more sensitive measure of small differences in δ-bond strength than does the metal–metal distance, or is this electronic transition influenced by effects not associated with metal–metal bonding?

There have been two previous attempts at correlating one or both of these spectral parameters with the extent of δ-bonding in quadruply bonded complexes. Sattelberger and Fackler (SF),[55] and subsequently other workers,[14,35,56,57] pointed out a nearly linear relationship between the metal–metal bond distance and the energy of the $^1(\delta \rightarrow \delta^*)$ band in several limited series of complexes. Specifically, those complexes with shorter metal–metal bonds, and thus presumably larger δ-overlaps, were observed to have higher energy $^1(\delta \rightarrow \delta^*)$ absorptions than did species with longer metal–metal bonds. A second, more comprehensive interpretation of the overall spectral behavior of these systems was offered by Manning and Trogler (MT).[52] On the basis of a valence-bond approach, these workers proposed that an increase in δ-overlap should result in a red shift of the $^1(\delta \rightarrow \delta^*)$ transition and a concomitant increase in its intensity. MT noted that overall, the spectral parameters of all quadruply bonded dimers formed such a trend: $^1(\delta \rightarrow \delta^*)$ bands at energies of greater than ~18 000 cm^{-1} were relatively weak ($\epsilon < 500$), and those at lower energies (~15–17000 cm^{-1}) were relatively intense ($1000 \leq \epsilon \leq 3500$).[51] That this general trend in spectroscopic behavior was, in fact, a manifestation of the magnitude of δ-overlap in these complexes was argued by pointing out that those species with the lowest energy and highest intensity absorptions were dimers of third-row transition metals or were complexes containing relatively strong electron-donating ligands (e.g., I^-, PR_3, CH_3^-), while high-energy, low-intensity $^1(\delta \rightarrow \delta^*)$ bands were found for complexes with "hard" ligands (^-O_2CR, SO_4^{2-}, H_2O) as well as for chromium dimers; from the standpoint of the effective charge on the dimetal unit, the former complexes would be expected to possess more diffuse atomic orbitals, and hence larger δ-overlaps, than would the latter species. The absence of an overall correlation of spectroscopic energy with metal–metal distance was rationalized by noting that since it is the σ- and π-interactions that largely determine the metal–metal distances found in quadruply bonded dimers, small differences in δ-bonding would not necessarily affect this bond distance.

While both of these proposals seem intuitively plausible, neither approach provides a totally satisfactory interpretation of the spectroscopic behavior of the $Mo_2X_4L_4$ compounds, nor do they appear to allow self-consistent correlations among the spectra of different subgroups of quadruply bonded complexes. Analysis of the electronic spectra of $Mo_2X_4(PMe_3)_4$, first within the MT framework,[52] leads to the conclusion that the 1400-cm^{-1} red shift and 60% increase in oscillator strength for the Cl, Br, I series is a manifestation of an increase in δ-overlap resulting from this perturbation. A semiquantitative estimate of the change in overlap (S) in this series, calculated[50] from these spectral parameters, yields $S(Mo_2Cl_4(PMe_3)_4) = 0.17$ and $S(Mo_2I_4(PMe_3)_4) = 0.23$; as was noted in the discussion of their molecular structures, some halogen dependence of the δ-bonding in these systems would not be unanticipated in view of the large difference in polarizability between chloride and iodide, and it is reasonable that a change in overlap of the magnitude inferred here would not affect the metal–metal distance. While the electronic structures of the $Mo_2X_4(PMe_3)_4$ complexes may indeed differ in exactly this manner, there are several pieces of evidence that suggest that such a conclusion cannot be drawn from this analysis of $^1(\delta \rightarrow \delta^*)$ energy and intensity. With respect to the δ-overlap-dependence of the transition energy, it has been previously demonstrated that complexes of the β-$Mo_2X_4(L-L)_2$ type that possess a bridging-phosphine-induced twisting about the metal–metal-bond axis, and hence reduced δ-overlap relative to eclipsed (0° twist angle) dimers,[58] show a $^1(\delta \rightarrow \delta^*)$ transition that systematically red-shifts, in contrast to the MT prediction, and loses intensity as the extent of δ-interaction decreases.[59,60] For example, the δ-overlap of β-$Mo_2Cl_4(dmpe)_2$ (dmpe = 1,2-bis(dimethylphosphino)ethane; twist angle = 40°) can be inferred to be no greater than 0.2 times that found in its eclipsed "rotamer", $Mo_2Cl_4(PMe_3)_4$;[58,60] the $^1(\delta \rightarrow \delta^*)$ band of the former complex is red shifted 4640 cm^{-1} relative to that of the latter and is an order of magnitude less intense (Table VII). The fact that the behavior of the spectroscopic parameters for the β-$Mo_2X_4(L-L)_2$ compounds (intensity decreases as the energy and δ-overlap decrease) runs opposite that observed overall for quadruply bonded dimers[51] (intensity increases as the energy decreases) suggests that the latter trend is probably not a direct manifestation of a variation in δ-interaction among these systems.

Examination of the spectra of the $Mo_2(O_2CR)_4$ systems,[51] which in the MT model should have among the smallest δ-overlaps, further emphasizes the discrepancies in this correlation. Even though the intensity of the $^1(\delta \rightarrow \delta^*)$ band of $Mo_2(O_2C$-n-$Pr)_4$ ($\bar{\nu}_{max} = 22700$ cm^{-1}, $\epsilon \sim 150$ M^{-1} cm^{-1})[61] is lower than that observed for β-$Mo_2Cl_4(dmpe)_2$, the $^2(\delta \rightarrow \delta^*)$ band of the one-electron-oxidized, $(\sigma^2\pi^4\delta^1)$-configured $Mo_2(O_2C$-n-$Pr)_4^+$ ion (the energy of which is a direct measure of the splitting of the one-electron δ and δ* levels in this system) is centered at 13 300 cm^{-1},[61] indicating that the energy of the δ/δ* orbital splitting ($E(\delta/\delta^*)$) is significantly larger for these species than those calculated for complexes with relatively intense ($\epsilon > 1000$) $^1(\delta \rightarrow \delta^*)$ absorptions ($Mo_2Cl_4(PH_3)_4$, $E(\delta/\delta^*) = 8070$;[28] $Mo_2Cl_8^{4-}$, 7900 cm^{-1} [62]), as

---

[53] Ziegler, T., personal communication. For further details on this calculation, see: Ziegler, T. *J. Am. Chem. Soc.* **1984**, *106*, 5901–5908.

[54] Lone pair ionization energies of homologous arsines and phosphines are generally similar (Elbel, S.; Tom Dieck, H. *Z. Naturforsch., B: Anorg. Chem., Org. Chem.* **1976**, *31B*, 178–189).

[55] Sattelberger, A. P.; Fackler, J. P. *J. Am. Chem. Soc.* **1977**, *99*, 1258–1259.

[56] Collins, D. M.; Cotton, F. A.; Koch, S.; Millar, M.; Murillo, C. A. *J. Am. Chem. Soc.* **1977**, *99*, 1259–1261. Cotton, F. A.; Koch, S.; Mertis, K.; Millar, M.; Wilkinson, G. *J. Am. Chem. Soc.* **1977**, *99*, 4989–4992.

[57] Bohmer, W. H.; Madeja, K.; Kurras, E.; Rosenthal, U. *Z. Chem.* **1978**, *18*, 453–454. Cotton, F. A.; Mott, G. N.; Schrock, R. R.; Sturgeoff, L. G. *J. Am. Chem. Soc.* **1982**, *104*, 6781–6782. Fanwick, P. E.; Bursten, B. E.; Kaufmann, G. B. *Inorg. Chem.* **1985**, *24*, 1165–1169.

[58] Campbell, F. L., III; Cotton, F. A.; Powell, G. L. *Inorg. Chem.* **1984**, *23*, 4222–4226.

[59] Campbell, F. L., III; Cotton, F. A.; Powell, G. L. *Inorg. Chem.* **1985**, *24*, 177–181.

[60] Hopkins, M. D.; Zietlow, T. C.; Miskowski, V. M.; Gray, H. B. *J. Am. Chem. Soc.* **1985**, *107*, 510–512.

[61] Hopkins, M. D., Ph.D. Thesis, California Institute of Technology, Pasadena, CA, 1986.

well as those estimated for compounds with "hard" ligands and weak ($\epsilon \sim 150$) absorptions[51] ($Mo_2(SO_4)_4^{4-}$, $E(\delta/\delta^*) = 8500$; $Mo_2(SO_4)_4^{3-}$, 7150 cm^{-1});[63] it is also in good agreement with theory ($Mo_2(O_2CH)_4$, $E(\delta/\delta^*) = 12\,180$ cm^{-1}).[6] Thus, the intensity of the $^1(\delta\to\delta^*)$ transition is clearly not directly proportional to $E(\delta/\delta^*)$.

Although the foregoing discussion indicates that the $^1(\delta\to\delta^*)$ energy tends to increase in tandem with δ-overlap, the above examples also show that this relationship is not as straightforward as the spectroscopic correlations pointed out by SF and others might suggest. These workers noted, for instance, that the red shift of this band (5200 cm^{-1}) for the $M_2(CH_3)_8^{n-}$ (M = Cr, Mo, Re, W)[55,56] complexes was monotonic with increasing bond distance ($\Delta d(W_2-Cr_2) = 0.28$ Å), in keeping with the notion that longer metal–metal distances imply relatively weaker δ-interactions. This $^1(\delta\to\delta^*)$ energy range is larger, however, than that found for $Mo_2Cl_4(PMe_3)_4$ and β-$Mo_2Cl_4(dmpe)_2$ (4640 cm^{-1}, Table VII), for which the corresponding difference in δ-overlap is known to be formally a factor of 5,[58-60] as well as for $Mo_2(O_2C$-*n*-$Pr)_4$ and $Mo_2(SO_4)_4^{4-}$ (3300 cm^{-1}),[51] whose one-electron-oxidized counterparts ($Mo_2(O_2C$-*n*-$Pr)_4^+$ and $Mo_2(SO_4)_4^{3-}$: vide supra) differ by nearly a factor of 2 in $E(\delta/\delta^*)$. From these data, the difference in δ-overlap between $W_2(CH_3)_8^{4-}$ and $Cr_2(CH_3)_8^{4-}$ that is inferred by the SF correlation appears to be unrealistically large for such closely related species. Furthermore, the fact that sizable spectroscopic shifts are observed between complexes that have very similar values of $E(\delta/\delta^*)$ (e.g., $Mo_2Cl_8^{4-}$, $Mo_2Cl_4(PMe_3)_4$),[64] as well as for those that have nearly identical metal–metal distances (e.g., $Mo_2X_4(PMe_3)_4$), suggests that this relationship of $^1(\delta\to\delta^*)$ energy to metal–metal distance is not likely to yield direct information about differences in δ-bonding among these systems.[65]

In formulating an answer to the question posed at the outset of this discussion, it is now clear that while the energy and intensity of the $^1(\delta\to\delta^*)$ band correlate well with δ-overlap in a few limited series of complexes, such as the torsionally distorted β-$Mo_2X_4(L-L)_2$ species, there are also numerous inconsistencies, the most notable of which appear to occur when comparisons, particularly of intensities, are attempted among complexes with different ligand sets. We initially noted that these spectral parameters reflect, to some extent, the magnitude of this metal–metal interaction for a given compound; the question raised by the preceding arguments thus concerns the origin of those contributions to the energy, and especially the intensity, of this transition that distort such spectroscopic correlations among complexes. While the data discussed herein do not, in general, corroborate the MT hypothesis, they strongly support the notion[52] that the nature of the ligands plays a central role in determining spectral intensity and energy. The fact that the distinct overall trend of increasing $^1(\delta\to\delta^*)$ intensity with decreasing transition energy that was noted by MT is not entirely attributable to systematic changes in metal–metal bonding suggests that these parameters may instead reflect strong *excited state* perturbations. Specifically, the mixing of $^1(\delta\to\delta^*)$ with high-oscillator-strength transitions of similar orbital character and symmetry would provide a mechanism through which intensity could be stolen; band positions would also reflect the coupling between these "zero-order" transitions.

We suggest that what the overall $^1(\delta\to\delta^*)$ spectral trend represents, as one proceeds from weak, high-energy $^1(\delta\to\delta^*)$ bands to intense, low-energy ones, is the gradual lowering in energy, for a given dimetal unit, of $\pi(\text{ligand}) \to \delta^*(M_2)$ transitions, and hence a concomitant increase in the extent of mixing between the $^1(\delta\to\delta^*)$ and $\pi(\text{ligand}) \to \delta^*(M_2)$ transitions.[66] Consequently, those compounds containing oxygen donors, which have relatively high energy LMCT bands, possess, regardless of δ-overlap, much weaker $^1(\delta\to\delta^*)$ bands ($\epsilon \leq 500$) than do halide-ligated dimers ($\epsilon \geq 1000$), for which LMCT transitions will be much lower in energy. The spectra of $Mo_2X_4(PMe_3)_4$ (Figure 4) provide an excellent example of this effect within a more restricted series of complexes. These species possess a $\pi(X) \to \delta^*(Mo_2)$ transition of the same symmetry ($b_1 \to a_2$; $^1B_2 \leftarrow {}^1A_1$) as $^1(\delta\to\delta^*)$; the calculated splitting of the $b_1(\pi(Cl))$ and $a_2(\delta^*(Mo_2))$ levels for $Mo_2Cl_4(PH_3)_4$ is between 30 000 and 36 000 cm^{-1},[28,53] placing this transition in the near-UV region. The dramatic increase in the intensity of the $^1(\delta\to\delta^*)$ band of these complexes according to Cl < Br < I is indicative of this transition progressively borrowing LMCT intensity, in agreement with the pronounced X → M red shift across this series (cf. band II). In contrast, the splitting of these orbitals for $Mo_2(O_2CH)_4$, a compound that is representative of the lower limit of $^1(\delta\to\delta^*)$ intensity,[66] is $\sim$63 000 cm^{-1}; the fact that $Mo_2(O_2C$-*n*-$Pr)_4$ and β-$Mo_2Cl_4(dmpe)_2$ have very similar $^1(\delta\to\delta^*)$ intensities, even though they nearly define the respective large and small δ/δ^*-splitting limits for d^4–d^4 complexes, is quite reasonable from the standpoint of this charge-transfer-mixing interpretation.[67]

Acknowledgment. We thank Dave Blair and Tad Fox for their experimental assistance. M.D.H. acknowledges the Sun Co. and Standard Oil Co. (Ohio) for providing graduate fellowships. M.J.B. was a participant in the Caltech Summer Undergraduate Research Program. This work was supported by National Science Foundation Grants CHE84-19828 (H.B.G.), CHE84-03836 (W.H.W.), and CHE82-19039 (CAD-4 diffractometer), and by the Exxon Education Foundation (W.P.S.). Work at Los Alamos National Laboratory was performed under the auspices of the U.S. Department of Energy.

Registry No. $Mo_2I_4(PMe_3)_4$, 89637-15-0; $Mo_2(O_2CCH_3)_4$, 14221-06-8; $Mo_2Br_4(PMe_3)_4$, 89707-70-0; $Mo_2Cl_4(AsMe_3)_4$, 105064-90-2; $K_4Mo_2Cl_8$, 25448-39-9; $Mo_2Cl_4(PMe_3)_4$, 67619-17-4; $W_2Cl_4(PMe_3)_4$, 73495-54-2; Me_3SiI, 16029-98-4; Me_3SiBr, 2857-97-8.

Supplementary Material Available: Tables of bond distances and bond angles, anisotropic thermal parameters, and calculated hydrogen atom positions for $Mo_2Br_4(PMe_3)_4$ and $Mo_2I_4(PMe_3)_4$ (7 pages); tables of observed and calculated structure factors (31 pages). Ordering information is given on any current masthead page.

---

(62) Norman, J. G., Jr.; Ryan, P. B. *J. Comput. Chem.* **1980**, *1*, 59–63.

(63) Hopkins, M. D.; Miskowski, V. M.; Gray, H. B. *J. Am. Chem. Soc.* **1986**, *108*, 959–963.

(64) $\Delta E(^1(\delta\to\delta^*)) = 1900$ cm^{-1}. $E(\delta/\delta^*)$ differs by less than 200 cm^{-1} between $Mo_2Cl_8^{4-}$ and $Mo_2Cl_4(PH_3)_4$.[28]

(65) Comparisons of the transition energies of the original SF series present a separate problem that has been discussed elsewhere,[59,60] namely that (in contrast to the β-$Mo_2X_4(L-L)_2$ complexes) contributions to the $^1(\delta\to\delta^*)$ energy arising from two-electron terms are not likely to remain constant over the range of metal–metal distances spanned by the $M_2(CH_3)_8^{n-}$ compounds.

(66) Charge-transfer transitions of the $\delta(M_2) \to \pi^*(\text{ligand})$ type will also be effective at intensity lending, provided they possess the correct symmetry for mixing with $^1(\delta\to\delta^*)$. It is because of this latter point that the $^1(\delta\to\delta^*)$ transitions of the $M_2(O_2CR)_4$ complexes are weak even though they are in close energetic proximity to intense MLCT bands (Santure, D. J.; Huffman, J. C.; Sattelberger, A. P. *Inorg. Chem.* **1985**, *24*, 371–378); theory indicates[6] that none of the low-lying MLCT states of these species has the correct symmetry for mixing.

(67) A detailed review of the theoretical aspects of the energies and intensities of $^1(\delta\to\delta^*)$ transitions is the subject of a separate report. Hopkins, M. D.; Miskowski, V. M.; Gray, H. B. *Polyhedron*, in press.